THE JOURNAL OF BIOLOGICAL CHEMISTRY VOL. 291, NO. 26, pp. 13743–13752, June 24, 2016

Dual Roles of *O*-Glucose Glycans Redundant with Monosaccharide *O*-Fucose on Notch in Notch Trafficking*

Received for publication, December 17, 2015, and in revised form, April 23, 2016 Published, JBC Papers in Press, April 25, 2016, DOI 10.1074/jbc.M115.710483

Kenjiroo Matsumoto[‡], Tomonori Ayukawa[§], Akira Ishio[§], Takeshi Sasamura[‡], Tomoko Yamakawa[‡], and Kenji Matsuno[‡1]

From the [‡]Department of Biological Sciences, Osaka University, 1-1 Machikaneyama, Toyonaka, Osaka 560-0043 and the [§]Department of Biological Science and Technology, Tokyo University of Science, 6-3-1 Niijuku, Katsushika-ku, Tokyo 125-1500, Japan

Notch is a transmembrane receptor that mediates cell-cell interactions and controls various cell-fate specifications in metazoans. The extracellular domain of Notch contains multiple epidermal growth factor (EGF)-like repeats. At least five different glycans are found in distinct sites within these EGF-like repeats. The function of these individual glycans in Notch signaling has been investigated, primarily by disrupting their individual glycosyltransferases. However, we are just beginning to understand the potential functional interactions between these glycans. Monosaccharide *O*-fucose and *O*-glucose trisaccharide (*O*-glucose-xylose-xylose) are added to many of the Notch EGF-like repeats. In *Drosophila*, Shams adds a xylose specifically to the monosaccharide *O*-glucose. We found that loss of the terminal dixylose of *O*-glucose-linked saccharides had little effect on Notch signaling. However, our analyses of double mutants of *shams* and other genes required for glycan modifications revealed that both the monosaccharide *O*-glucose and the terminal dixylose of *O*-glucose-linked saccharides function redundantly with the monosaccharide *O*-fucose in Notch activation and trafficking. The terminal dixylose of *O*-glucose-linked saccharides and the monosaccharide *O*-glucose were required in distinct Notch trafficking processes: Notch transport from the apical plasma membrane to adherens junctions, and Notch export from the endoplasmic reticulum, respectively. Therefore, the monosaccharide *O*-glucose and terminal dixylose of *O*-glucose-linked saccharides have distinct activities in Notch trafficking, although a loss of these activities is compensated for by the presence of monosaccharide *O*-fucose. Given that various glycans attached to a protein motif may have redundant functions, our results suggest that these potential redundancies may lead to a serious underestimation of glycan functions.

In transmembrane receptors, glycan modifications play important roles in the receptors' maturation, transport, and physical interactions with ligands (1–4). Various types of glycosylation are often found on small protein motifs, and the specific functions of these glycosylation events are usually analyzed by disrupting individual glycans (5). However, the functional interactions between these various glycans are not well understood.

The evolutionarily conserved Notch receptors typically contain 36 epidermal growth factor (EGF)[2]-like repeats, which bind transmembrane ligands from the Delta and Serrate families (6). Notch signaling functions in a broad spectrum of cell specification processes through local cell-cell interactions (7). At least five different glycan modifications have been found on the Notch EGF-like repeats: *N*-linked glycan modifications (8) and four *O*-linked glycan modifications: *O*-fucose (9–11), *O*-glucose (12, 13), *O*-GlcNAc (14), and *O*-GalNAc (15). A potential *O*-xylosylation of the EGF-like repeats has also been observed *in vitro* (16). The individual modifications have been analyzed to determine their specific functions and generate a model for how glycosylation regulates receptor functions (8–15). For example, *O*-fucosyltransferase 1 (*O*-fut1) adds *O*-fucose to a C2*XXXX*(S/T)C3 motif in the EGF-like repeats (Fig. 1*A*) (9, 10). Fringe, a β1,3 *N*-acetylglucosaminyltransferase, adds GlcNAc to the *O*-fucose (11); this GlcNAc modification changes the binding preference of Notch for different ligand types (9–11, 17). The function of the monosaccharide *O*-fucose was previously unclear, because *O*-fut1 has dual functions: an *O*-fucosyltransferase function and a Notch-specific chaperone-like function apparently independent of its *O*-fucosyltransferase activity (18). However, it was recently found that the monosaccharide *O*-fucose is essential for Notch signaling at high temperatures (30 °C) (19). Rumi adds *O*-glucose to a C*XSX*(P/A)C motif in the EGF-like repeats, and this modification is also essential for Notch activation (Fig. 1*A*) (12). Shams adds a xylose to this monosaccharide *O*-glucose, and this xylosylation negatively regulates Notch signaling (Fig. 1*A*) (13).

Recently, it was suggested that the monosaccharide *O*-fucose and the *O*-glucose trisaccharide function redundantly in Notch signaling, probably by promoting the proper folding of Notch (19). Defects associated with the simultaneous loss of these two modifications are far more severe than and qualitatively different from the loss of only one of the modifications (19). How-

* This work was supported by grants-in-aid from the Japanese Ministry of Education, Culture, Sports, and Science (to K. Matsuno), grants from PRESTO, the Japan Science and Technology Agency (to K. Matsuno), the Japan Society for the Promotion of Science (to K. Matsumoto), the Naito Foundation (to K. Matsumoto), and a research grant (2015) from the Mizutani Foundation for Glycoscience (to K. Matsuno). The authors declare no that they have no conflict of interest with the contents of this article.

[1] To whom correspondence should be addressed. Tel.: 81-6-6850-5804; Fax: 81-6-6850-5805; E-mail: kmatsuno@bio. sci.osaka-u.ac.jp.

[2] The abbreviations used are: EGF, epidermal growth factor; *D*E-Cad, *D*E-cadherin; ER, endoplasmic reticulum; GlcNAc, *N*-acetylglucosamine; NICD, Notch intracellular domain; NECD, Notch extracellular domain; *O*-fut1, *O*-fucosyltransferase 1; Sens, Senseless; SOP, sensory organ precursor; Wg, Wingless; Uxs, UDP-xylose synthase; Ap, apterous; GAG, glycosaminoglycan; AJ, adherens junction; PDI, protein-disulfide isomerase.

ever, the specific sugar moiety in the *O*-glucose trisaccharide that functions redundantly with *O*-fucose was previously unknown. In this study, taking advantage of *Drosophila* genetics, we addressed this question by combining various mutations that affect these two glycan modifications. We here revealed that the terminal dixylose and *O*-glucose have distinct roles in Notch transport, both of which are redundant with the roles of *O*-fucose.

Experimental Procedures

Drosophila Strains—We used Canton-S as the wild-type strain. The following mutant alleles were used: *O-fut1*^{R245A} (19); the previously described *sham*-null allele *shams*^{34} (13), the *UDP-xylose synthase* (*Uxs*)-null allele *Uxs*^{1} (this study), the *Uxs*-deletion mutant *Df(2R)BSC783* (Bloomington 27355) (20), and the *rumi*-null allele *rumi*^{44} (12). The following UAS lines were used for RNA interference (RNAi): UAS-*Notch* inverted repeat (21) and UAS-*peptide O-xylosyltransferase* (*Oxt*) inverted repeat (21). As lines expressing Gal4 specifically in the dorsal side of the wing disc, posterior side of wing disc, eye, and bristles on the dorsal head capsule, *apterous* (*ap*)-*Ga4* (23), *hedgehog (hh)-Gal4* (24), *GMR-Gal4* (25), and *scabrous* (*sca*)-*Gal4* (26) were used, respectively.

Generation of Uxs^{1}—To generate a null allele of *Uxs*, we deleted the genomic *Uxs* gene by imprecise excision of a P-element inserted into the *Uxs* locus of *P{EPgy2}CG7979EY00136* (Bloomington stock number 15001) using a standard procedure (27). We mobilized the P-element by crossing *P{EPgy2}CG7979EY00136* with *w**; *Dr*^{1}/*TMS, P{ry*$^{+t7.2}$ *= Delta2–3}99B* (Bloomington stock number 1016). The genomic DNA was purified from the potential deletion-mutant lines, and the deletion was detected by PCR using the forward primer 5′-GAGCTGTAACCTGCAAGAAGTC-3′ and the reverse primer 5′-CACATTTCTGGATCTCAGCTAG-3′. We obtained *Uxs*^{1} and confirmed the deletion by sequencing the genomic DNA.

Immunostaining—Drosophila wing discs were immunostained as described previously (28), except for the 3G10 and 2H antibody staining. Briefly, for most antibody stainings, the wing discs were dissected from third-instar larvae in PBS and fixed in PLP fixing solution (2% paraformaldehyde, 0.01 M $NaIO_4$, 0.075 M lysine, 0.037 M sodium phosphate, pH 7.2) for 40 min at room temperature. The wing discs were washed three times in PBS-DT (0.3% sodium deoxycholate, 0.3% Triton X-100 in PBS) and incubated in PBS-DT with the primary antibody at 4 °C overnight. The wing discs were then washed three times in PBS-DT, and incubated in PBS-DT with the secondary antibody at room temperature for 2 h. The wing discs were then washed three times in PBS-DT and observed with an LSM700 confocal microscope. For the 3G10 antibody staining, the fixed wing discs were incubated with 400 milliunits of heparinase III (New England Biolabs) for 4 h at 37 °C (29, 30). For staining with the 2H (C458.2H) antibody, which recognizes the Notch extracellular domain, the fixed wing discs were then washed in PBS (without detergent) and incubated with the 2H antibody for 2 h at room temperature. The wing discs were washed in PBS and fixed again. The wing discs were then washed in PBS, 0.5% Tween 20 (0.5% Tween 20 in PBS) and stained with an anti-GFP antibody. Finally, the wing discs were washed in PBS, 0.5% Tween 20 and treated with the secondary antibody.

The following antibodies were used at the indicated concentrations: mouse anti-NECD monoclonal antibody (1:100; C458.2H (2H); from the Developmental Studies Hybridoma Bank (DSHB)) (19), mouse anti-NICD monoclonal antibody (1:1000; C17.9C6; DSBC) (19), rat anti-NICD polyclonal antibody (1:1000; gifted by Dr. Spyros Artavanis-Tsakonas) (19), mouse anti-Wg monoclonal antibody (1:20; 4D4; DSBC) (28), rat anti-Cadherin monoclonal antibody (1:20; 7E8A10; DSBC) (19), guinea pig anti-Senseless polyclonal antibody (1:1000; gifted by Dr. Hugo Bellen) (19), rabbit anti-GFP polyclonal antibody (1:500; MBL), and Alexa 488-, Cy3-, and Cy5-conjugated affinity-purified donkey secondary antibodies (28) (1:500; Jackson). The epitope of the 2H antibody is EGF repeats 12–20 in the extracellular domain of Notch, and the epitope of C17.9C6 is the intracellular domain of Notch (19).

In Situ Hybridization—In situ hybridization to detect the *wingless* (*wg*) transcript was performed as described previously (31). Briefly, a *wg* cDNA was used as a template to synthesize RNA probes (32). T7 and SP6 promoters were added to the 5′- and 3′-ends of the *wg* cDNA by PCR using a forward primer (5′-AAATAATACGACTCACTATAGGGATGCGTGGAAAACTTACAAG-3′) and a reverse primer (5′-AAACTATAGTGTGTCACCTAAATCGCATTCGATTTTTCTGC-3′). A digoxigenin-labeled *wg* RNA probe was synthesized from this template using the DIG RNA labeling mix (Roche Applied Science). The SP6 and T7 RNA polymerases were used to make antisense and sense probes, respectively.

Generation of Somatic Mosaic Clones—Somatic clones of *O-fut1*^{R245A}, *rumi*^{44}, and *shams*^{34} were generated by FLP-FRT recombination in the wing discs of third-instar larvae. FLP recombinase mediates site-specific recombination between FRT (FLP recombinase target) sites (33, 34). The FLP-mediated recombination between FRT sites in each homologous chromosome generates mitotic clones homozygous for a mutation in cells heterozygous for it (33, 34). The following fly genotypes were used: *y w Ubx-FLP*; *FRTG13 O-fut1*^{R245A}*/FRTG13 Ubi-GFP, y w Ubx-FLP*; *shams*^{34} *FRT82B/Ubi-GFP FRT82B, Ubx-FLP*; *Ubi-GFP*; *FRT82B/shams*^{34}, *FRT82B, Ubx-FLP*; *Ubi-GFP*; *FRT82B/rumi*^{44}, *FRT82B, Ubx-FLP*; *FRTG13 O-fut1*^{R245A}*/FRTG13 Ubi-GFP*; *FRT82B shams*^{34}, and *Ubx-FLP*; *FRTG13 O-fut1*^{R245A}*/FRTG13 Ubi-GFP*; *FRT80B rumi*^{44}, as described previously (33, 34).

Results

CG7979 Encodes a Drosophila UDP-xylose Synthase—The terminal dixylose of *O*-glucose-linked saccharides negatively regulates Notch signaling in a tissue-specific manner (13), as shown by loss- and gain-of-function analyses of the *shams* gene, which encodes the *O*-glucose-specific xylosyltransferase (13). However, this negative regulation may not be due to Shams' xylosyltransferase activity, given the controversy of the role of the *O*-fucosyltransferase *O*-fut1. The essential role of *O*-fut1 in Notch signaling was first proposed to be independent of its enzymatic activity (18, 35), but a recent study indicated that enzymatic activity of *O*-fut1 is essential in Notch signaling (19). Thus, before addressing the functions of the terminal dixylose

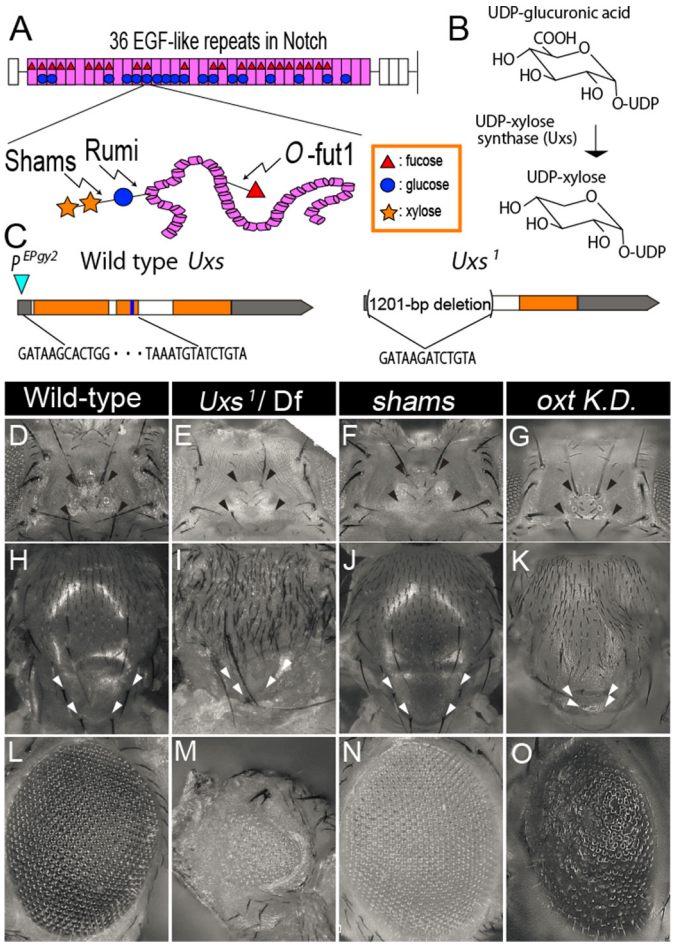

FIGURE 1. **Overlaps in the *Uxs*-mutant, *shams*-mutant, and *oxt* knockdown phenotypes.** *A, upper*: schematic of the EGF-like repeats in Notch, showing the *O*-glucose trisaccharide and monosaccharide *O*-fucose. The extracellular domain of *Drosophila* Notch has 36 EGF-like repeats (*pink*); 23 can be *O*-fucosylated (*red triangles*) and 18 can be *O*-glucosylated (*blue circles*). *Lower*: *O*-fucose (*red triangle*) is added by *O*-fut1. During the synthesis of the *O*-glucose trisaccharide (*O*-glucose-xylose-xylose), the *O*-glucose (*blue circle*) and first xylose (*yellow star*) are added by Rumi and Shams, respectively. *B*, schematic of UDP-xylose biosynthesis. Uxs is an essential enzyme for the *de novo* synthesis of UDP-xylose in *Drosophila*. *C*, genomic organization of the *Drosophila Uxs* locus, showing the untranslated (*gray*) and protein-coding (*orange*) regions of the *Uxs* gene exon, introns (*white*), and the region encoding a nucleotide-binding site (*blue*). A P-element (EPgy2) insertion site is indicated by a *blue triangle*. The 1201-bp deletion in Uxs^1 is indicated by *parentheses*; the end points are shown by the DNA sequence. *D-O*, phenotypes of the head (*D–G*), notum (*H–K*), and eye (*L–O*) of wild-type (*D*, *H*, and *L*), and $Uxs^1/Df(3L)Exel6112$ (*E*, *I*, and *M*) and $shams^{34}$ homozygotes (*F*, *J*, and *N*), and *oxt* knockdown flies (*G*, *K*, and *O*). Missing ocellar and post-vertical bristles are indicated by *black* (*D–G*) and *white* (*H–K*) *arrowheads*, respectively. *sca-Gal4* (*G*), *ap-Gal4* (*K*), or *GMR-Gal4* (*O*) were used for the *oxt* knockdown.

of *O*-glucose-linked saccharides, it is important to confirm that phenotypes associated with *shams* mutations are indeed due to the absence of the terminal dixylose of *O*-glucose-linked saccharides. Therefore, we attempted to abolish the xylosylatin of Notch by mutating a different gene in *Drosophila*.

UDP-xylose, which is essential for xylosylation as the xylose donor, is synthesized from UDP-glucuronic acid (36) (Fig. 1*B*). In mammals, UDP-xylose synthesis fully depends on *UDP-xylose synthase 1*, which encodes their only UDP-xylose synthase (37). The *Drosophila* ortholog of *UDP-xylose synthase 1* is *UDP-xylose synthase* (*Uxs*; *CG7979*), the only gene in the *Drosophila* genome that encodes UDP-xylose synthase (38). To generate potential *Uxs*-null mutants, we used imprecise P-element excision. Excising the P-element from the $\{EPgy2\}CG7979^{EY00136}$ line produced the *Uxs*-deletion mutant Uxs^1 (Fig. 1*C*). The Uxs^1 mutant has a 1201-base pair deletion of the *Uxs* genomic DNA locus, which removes its putative initiation codon and more than half of its coding region, corresponding to the N-terminal half of the Uxs protein (including a nucleotide-binding site) (38) (Fig. 1*C*). The molecular changes in the Uxs^1 mutant suggest that it is a null-mutant allele of *Uxs*.

To analyze the defects associated with this *Uxs* mutation, we observed the phenotypes of the Uxs^1 mutant. To avoid observing phenotypes associated with potential background mutations, we also analyzed a trans-heterozygote of Uxs^1 and *Deficiency* (*Df*) *f(3L)Exel6112*, a previously reported deletion mutant uncovering the *Uxs* locus (20). These phenotypes were essentially the same as those of the Uxs^1 homozygote, further indicating that Uxs^1 is a null allele. We also compared these phenotypes with *shams* mutants, in which the *O*-glucose attached to the Notch EGF-like repeats is not xylosylated (13). We found that the trans-heterozygotes of Uxs^1 and *Df(3L)Exel6112* was lethal at the late pupal stage, although pharate adults (adults that died before emerging from the pupal case) were occasionally obtained (Fig. 1, *E*, *I*, and *M*). In contrast, homozygous *sham*-null mutants are viable, as previously described (Fig. 1, *F*, *J*, and *N*), indicating that the Uxs^1-mutant defects are more severe than those in *shams* mutants (13). We found that all of the trans-heterozygotes of Uxs^1 and *Df(3L)Exel6112* pharate adults examined ($n = 14$) were missing bristles on the dorsal head capsule (Fig. 1*E*); this phenotype was also found in the *shams* mutants ($n = 22$) (Fig. 1*F*), as previously observed (13). This overlap in phenotypes between Uxs^1 and *shams* mutants appears consistent with our hypothesis that both genes are required for the xylosylation of *O*-glucose on Notch EGF-like repeats. In addition, the Uxs^1 mutants ($n = 14$) had a rough-eye phenotype and were missing scutellum bristles (Fig. 1, *I* and *M*); these defects were not present in the *shams* mutants ($n = 22$) (Fig. 1, *J* and *N*). We speculated that these phenotypes might result from defects in glycosaminoglycans (GAG) synthesis, which requires UDP-xylose (39).

GAG synthesis begins with the *O*-xylosylation of core proteins by *O*-xylosyltransferase (40). Thus, GAG synthesis is probably abolished in the Uxs^1 mutant due to the absence of UDP-xylose. We detected GAG by a specific antibody against the 3G10 epitope, which is exposed after GAG is digested by heparinitase (29, 30). GAG staining was largely abolished in all of the wing discs in trans-heterozygotes of Uxs^1 and *Df(3L)Exel6112* ($n = 23$) (Fig. 2, *C* and *D*) compared with wild-type wing discs ($n = 27$) (Fig. 2, *A* and *B*). Mutants of other genes required for GAG synthesis and maturation, such as *toutvelu* and *sulfateless*, are also recessive lethal at the same developmental stage as Uxs^1, which supports our idea that GAG synthesis is disrupted in the Uxs^1 mutant (29, 41).

Oxt is another enzyme required for GAG synthesis (38). Although an *oxt* mutant has not been reported, the knockdown of *oxt* in *Drosophila* by RNA interference was reported (22). As reported before, the knockdown of *oxt* resulted in a rough eye phenotype ($n = 26$) (Fig. 1*O*) (22). Here, we found that the knockdown of *oxt* also resulted in bristle loss in the scutellum

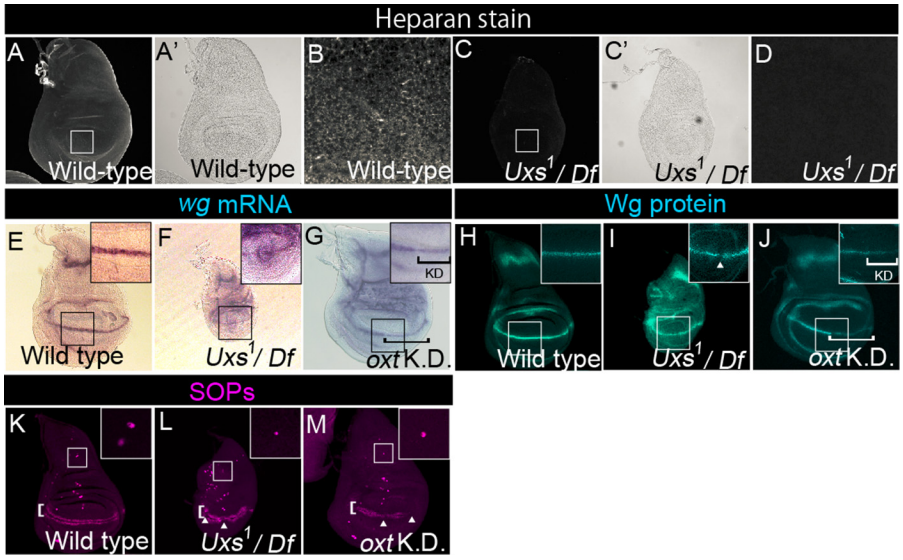

FIGURE 2. **Notch-signaling activation is normal in the *Uxs* mutant.** *A–D,* wild-type (*A*, *A′*, and *B*) and *Uxs*^{1}*/Df(3L)Exel6112* (*C*, *C′*, and *D*) wing discs stained with an anti-heparan sulfate antibody. *A′* and *C′* show optic microscope images of *A* and *C*, respectively. *B* and *D* show magnified views of the *white squares* in *A* and *C*, respectively. *E-G*, expression of *wg*, detected by *in situ* hybridization (*magenta*) in wild-type (*E*), *Uxs*^{1}*/Df(3L)Exel6112* (*F*), and *oxt* knockdown (*G*) wing discs. *Insets* show magnified views of the *black squares*. *Black bracket* in *G* indicates the *oxt* knockdown region. *H–J,* distribution of Wg protein, detected by anti-Wg antibody staining (*blue*) in wild-type (*H*), *Uxs*^{1}*/Df(3L)Exel6112* (*I*), and *oxt* knockdown (*J*) wing discs; *insets* show magnified views of the *white squares*. *White arrowhead* indicates a gap between Wg protein-expressing cells along the boundary of the dorsal and ventral compartments. *White bracket in J* indicates the *oxt* knockdown region. *K–M,* SOPs detected by anti-Sens antibody staining (*magenta*) in wild-type (*K*), *Uxs*^{1}*/Df(3L)Exel6112* (*L*), and *oxt* knockdown (*M*) wing discs. *White arrowheads* in *L* and *M* indicate gaps between *Sens*-expressing cells along the boundary (*white brackets*) between the dorsal and ventral compartments. *Insets* show magnified views of the areas outlined in *white*, which contain SA neuron precursors. All wing discs were isolated from third-instar larvae cultured at 25 °C except in the RNAi analysis. *hh-Gal4* (*G* and *J*) or *ap-Gal4* (*M*) was used for the *oxt* knockdown. All of the *oxt* knockdown wing discs were isolated from third-instar larvae cultured at 30 °C.

($n = 21$) (Fig. 1*K*), but not on the dorsal head capsule ($n = 28$) (Fig. 1*G*). Thus, within the limits of RNAi analysis, these results suggest that the bristle loss in the scutellum and rough eye found in the *Uxs*-mutant or *oxt* knockdown flies may have been due to the disruption of GAG synthesis, whereas the loss of bristles on the dorsal head capsule found in the *Uxs-* or *shams*-mutant flies may have been due to loss of the terminal dixylose of *O*-glucose-linked saccharides.

Wg Signaling Is Decreased in the Uxs Mutant—Previous analysis of the shams mutant showed that the terminal dixylose of *O*-glucose-linked saccharides on the EGF-like repeats of Notch negatively regulates Notch signaling in a tissue-specific manner, although the *shams* mutant phenotype suggested that hyper-activation of the Notch signaling was subtle (13). Thus, we used the *Uxs* mutant to re-examine potential roles of the terminal dixylose of *O*-glucose-linked saccharides in other developmental processes controlled by Notch signaling. The expression of *wingless* (*wg*), which is activated by Notch signaling along the boundary of the dorsal and ventral compartments in the third-instar wing disc (42), was analyzed by *in situ* hybridization in a *Uxs*-mutant trans-heterozygote of *Uxs*^{1} and *Df(3L)Exel6112* (Fig. 2*F*). Although the *wg* expression may have been slightly reduced in the *Uxs*-mutant wing discs, the pattern of expression was not markedly different from wild-type, indicating that the Notch-signaling activity was not severely affected in any of the wing discs examined ($n = 19$) (compare Fig. 2, *E* and *F*). Similarly, *wg* expression was slightly reduced in the region of the wing discs where the *Oxt* gene was knocked down by RNAi ($n = 36$) (Fig. 2*G*). In addition, the amount of Wg protein was slightly reduced and distributed more diffusely in all of the *Uxs*-mutant wing discs ($n = 23$) and in 77% of the *Oxt* knockdown wing discs ($n = 31$) (Fig. 2, *I* and *J*). Similar abnormalities in Wg protein distribution were reported in mutants with defective GAG synthesis (43). Wg gradient is modulated by GAG, through the binding between Wg and GAG (44). In addition, the array of sensory organ precursors (SOPs) expressing *senseless* (*sens*), which depends on Wg signaling, along the boundary of the dorsal and ventral compartments was interrupted in these wing discs (45, 46) (compare Fig. 2, *K–M,* and see *arrowheads* in Fig. 2, *L* and *M*). Therefore, Wg signaling is decreased in the *Uxs*-mutant and *oxt* knockdown wing discs, probably due to disrupted GAG synthesis. This reduction in Wg signaling may also account for the apparent slight reduction in *wg* expression we observed in the *Uxs* mutant and *oxt* knockdown wing discs (Fig. 2, *F* and *G*) (45, 46).

O-Fucose and the Terminal Dixylose of O-Glucose-linked Saccharides on Notch EGF-like Repeats Play Redundant Roles in Notch Signaling Activation—The number of SOPs in wing discs is restricted by lateral inhibition though Notch signaling (47). Knocking down *Notch* significantly increased the number of SOPs, which subsequently formed SA neurons (compare Figs. 2*K*, 3*A*, and 4). However, the number of SOPs in *Uxs* or *shams*-mutant wing discs was comparable with that in wild-type at 25 °C (compare Fig. 2, *K* and *L*, and 3, *E,* and see Fig. 4). Therefore, Notch signaling is not notably altered in the absence of the terminal dixylose of *O*-glucose-linked saccharides. However, we previously found that monosaccharide *O*-fucose and *O*-glucose trisaccharide on Notch EGF-like repeats have redundant roles in Notch trafficking and Notch-signaling activation (19). Thus, although the loss of only the terminal dixylose of *O*-glucose-linked saccharides did not significantly affect Notch

signaling, it was possible that the concurrent loss of monosaccharide *O*-fucose and the terminal dixylose of *O*-glucose-linked saccharides could cause defects in Notch signaling.

To address this possibility, we examined the effect of this xylosylation on Notch signaling in the absence of *O*-fucosylation. *O-fut1*^{R245A} encodes a mutant form of *O*-fut1 protein that largely lacks *O*-fucosyltransferase activity but maintains a Notch-specific chaperone-like function that is independent of its enzymatic activity (18, 19). Thus, although the Notch protein synthesized in the *O-fut1*^{R245A} mutant lacks the *O*-fucose modification, the Notch protein is folded within the scope of the *O*-fut1 chaperone-like function. The number of SOPs was not significantly affected in *O-fut1*^{R245A} homozygote wing discs at 25 °C (permissive temperature) (Figs. 3*B* and 4), although the number increased markedly at 30 °C (non-permissive temperature) (Figs. 3*J* and 4), as previously reported (19). However, in this study, to compare effects on Notch signaling under the same conditions, all other experiments were conducted at 25 °C. In the *O-fut1*^{R245A} and *Uxs*^{1} double-homozygote wing discs, the number of SOPs was not affected at 25 °C (Figs. 3*C* and 4). However, in *O-fut1*^{R245A} homozygotes combined with *Uxs*^{1} heterozygotes, the number of SOPs increased significantly at 25 °C (Figs. 3*D* and 4). This discrepancy can be explained if the Wg signal-dependent induction of SOP fate, which occurs prior to its lateral inhibition, was disrupted in the *Uxs*^{1} homozygote at 25 °C. In this case, the fate of SOP might be induced normally in the *Uxs*^{1} heterozygote wing discs, but a subsequent failure of the typical Notch signal-dependent lateral inhibition increases the number of SOPs. This idea was further supported by our analysis of *O-fut1*^{R245A} mutant wing discs in combination with *shams*-mutant wing discs, in which Wg signaling is normal (13). The number of SOPs increased significantly in the wing discs of a *O-fut1*^{R245A} and *shams* double homozygote at 25 °C (Figs. 3*F* and 4). These findings indicated that the terminal dixylose moiety of *O*-glucose glycans and the *O*-fucose monosaccharides on Notch function redundantly in Notch-signaling activation.

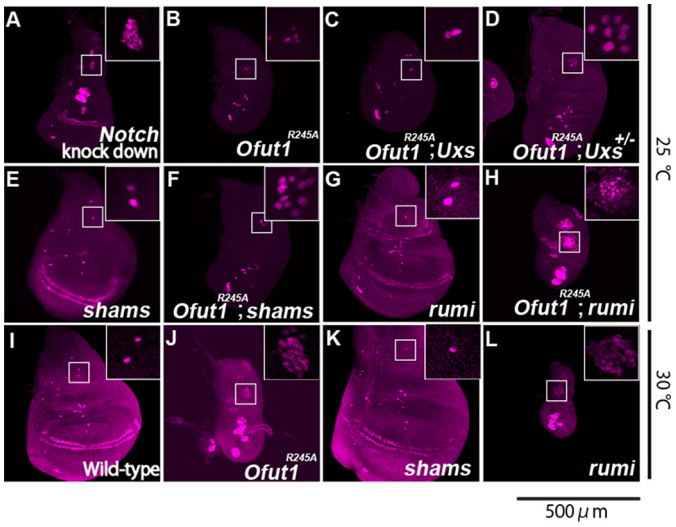

FIGURE 3. **The *O*-glucose trisaccharide plays multiple roles in Notch-signaling activation and shows redundancy with monosaccharide *O*-fucose.** *A–L*, SOPs in wing discs were detected by anti-Sens antibody staining (*magenta*). *A–H*, wing discs from a *Notch* knockdown (*A*), *O-fut1*^{R245A} homozygote (*B*), *O-fut1*^{R245A} and *Uxs*^{1} double homozygote (*C*), *O-fut1*^{R245A}/*O-fut1*^{R245A}; *Uxs*/+ (*D*), *shams* homozygote (*E*), *O-fut1*^{R245A} and *shams*^{34} double homozygote (*F*), *rumi*^{44} homozygote (*G*), and *O-fut1*^{R245A} and *rumi*^{44} double homozygote (*H*); the wing discs were isolated from larvae raised at 25 °C. *I–L*, wing discs from wild-type (*I*), *O-fut1*^{R245A} homozygote (*J*), *shams* homozygote (*K*), and *rumi*^{44} homozygote (*L*) *Drosophila*; wing discs were isolated from third-instar larvae raised at 30 °C. *Insets* show magnified views of the areas in *white squares*, which contained SA-neuron precursors. The *scale bar* is 500 μm and applicable for all panels.

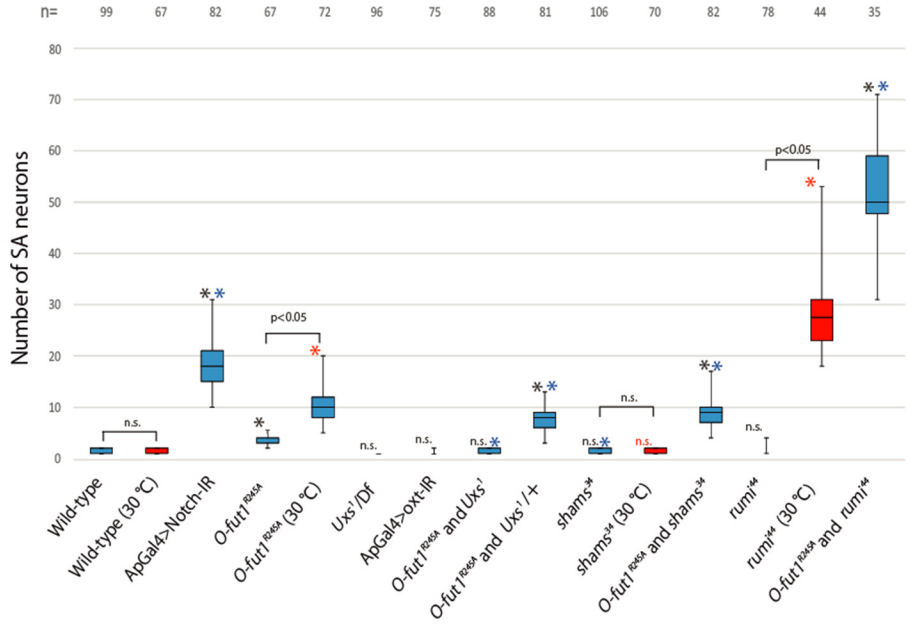

FIGURE 4. **The number of SA neurons in various single and double mutants.** Box plots of the number of SA neurons (*vertical axis*) for each genotype (across the *bottom*). Representative results are shown in Figs. 2 and 3. SA neurons were identified by anti-Sens antibody staining in wing discs isolated from third-instar larvae raised at 25 °C (*blue boxes*) or 30 °C (*red boxes*); *black asterisks* and *n.s.* indicate: *, $p < 0.05$ and no significant difference, respectively, compared with wild-type at 25 °C. *Blue asterisks* indicate: *, $p < 0.05$ compared with *O-fut1*^{R245A} homozygotes at 25 °C. *Red asterisks* and *n.s.* indicate: *, $p < 0.05$ and no significant difference, respectively, compared with wild-type at 30 °C. The number of wing discs analyzed in each experiment (biological replicates) is shown at the *top* of the graph. Each experiment was done three times.

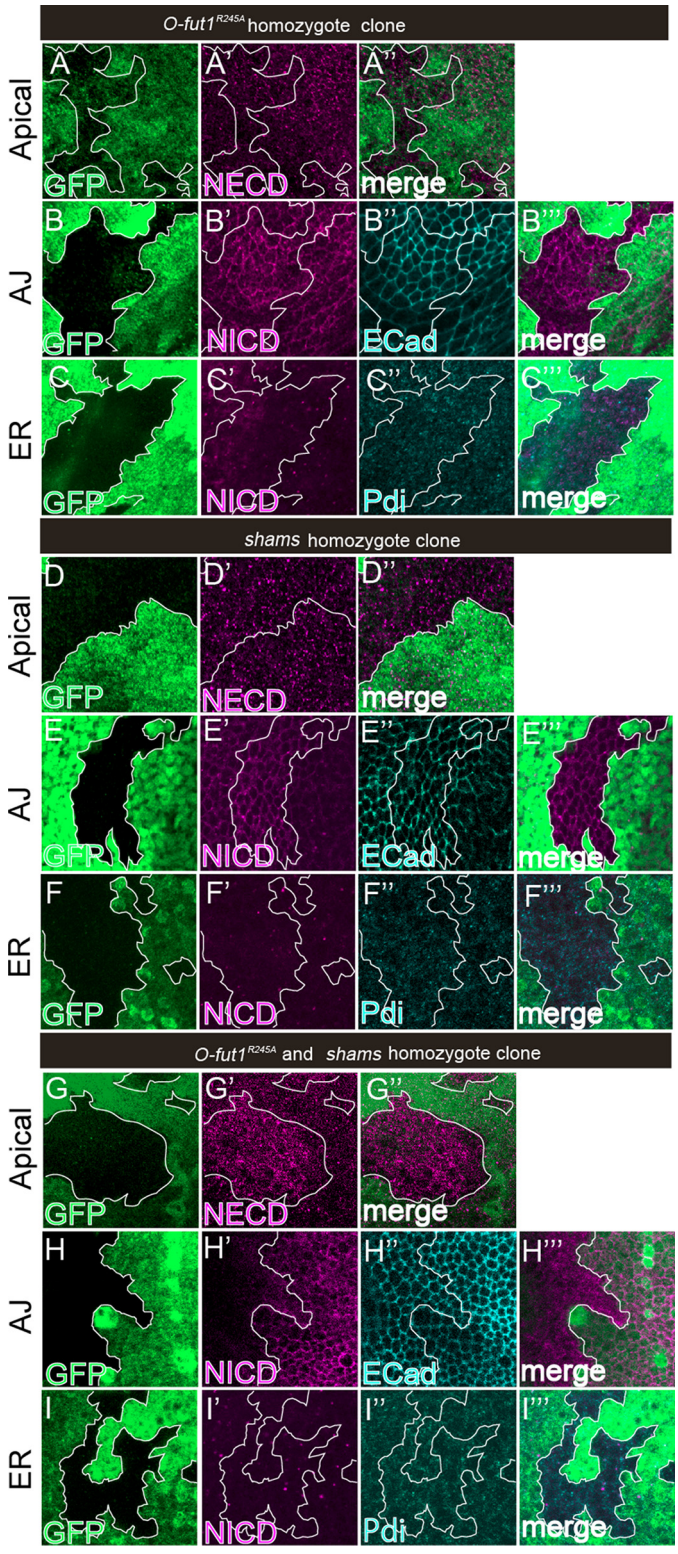

FIGURE 5. **Monosaccharide *O*-fucose and terminal dixylose of *O*-glucose-linked saccharides play redundant roles in relocating Notch from the apical plasma membrane to AJs.** *A–I‴*, wing discs with somatic clones homozygous for *O-fut1*^{R245A} (*A–C‴*) and *shams* (*D–F‴*) or double-homozygous for *O-fut1*^{R245A} and *shams* (*G–I‴*) were stained with antibodies against NECD (*A′*, *A″*, *D′*, *D″*, *G′*, and *G″*); NICD (*B′*, *B‴*, *C′*, *C‴*, *E′*, *E‴*, *F′*, *F‴*, *H′*, *H‴*, *I′*, and *I‴*); *D*E-cad (*B″*, *E″*, and *H″*); and PDI (*C″*, *C‴*, *F″*, *F‴*, *I″*, and *I‴*). Optical images show planes corresponding to the apical membrane (*A–A″*, *D–D″*, and *G–G″*); AJs (*B–B‴*, *E–E‴*, and *H–H‴*); and the medial region including the ER (*C–C‴*, *F–F‴*, and *I–I‴*). Note that NECD staining was increased at the apical membrane (*G′*), and NICD staining was abolished at the AJs (*H′*) in the *O-fut1*^{R245A} and *shams* double-homozygous cells (lacking GFP). Mosaic clones of mutant cells are indicated by the absence of GFP. Clone boundaries are indicated by *white lines*. Wing discs were isolated from larvae raised at 25 °C. *A″*, *B‴*, *C‴*, *D″*, *E‴*, *F‴*, *G″*, *H‴*, and *I‴* show merged images from *A* and *A′*, *B* and *B′*, *C–C″*, *D* and *D′*, *E* and *E′*, *F–F″*, *G* and *G′*, *H* and *H′*, and *I-I″*, respectively.

Monosaccharide O-Fucose and the Terminal Dixylose of O-Glucose-linked Saccharides Function Redundantly in Notch Trafficking—To investigate the cause of the reduction in Notch signaling associated with the concurrent loss of *O*-fucose and the terminal dixylose of *O*-glucose-linked saccharides, we examined Notch trafficking. *O*-Fucose and *O*-glucose trisaccharide contribute to normal Notch trafficking in a temperature-dependent manner; Notch trafficking is defective at 30 °C (non-permissive temperature) but largely normal at 25 °C (permissive temperature) (12, 13, 19). Using the FLP/FRT system, we generated somatic mosaics of *O-fut1*^{R245A} or *shams*-mutant cells, or *O-fut1*^{R245A} and *shams* double-mutant cells; the mutant cells were identified by the absence of *GFP* expression in the wing discs. In these experiments, Notch protein localized to the apical plasma membrane, adherens junctions (AJs), and endoplasmic reticulum (ER) was analyzed at 25 °C. Notch at the apical plasma membrane was specifically detected by an anti-Notch extracellular domain antibody (NECD) in non-permeabilized wing discs (19). Notch localized normally to the apical plasma membrane in mutant cells of either *O-fut1*^{R245A} (n = 23) or *shams* (n = 24) in all cases (Fig. 5, *A-A″* and *D–D″*). However, in *O-fut1*^{R245A} and *shams* double-mutant cells, Notch showed excessive accumulation at the apical plasma membrane in all cases (n = 19) (Fig. 5, *G–G″*). In permeabilized epithelial cells, Notch protein detected by an anti-Notch intracellular domain antibody (NICD) localized predominantly to the AJs, as reported previously (48, 49). In these experiments, AJs were detected by staining with an anti-*Drosophila* E-Cadherin (*D*E-cad) antibody (48, 49). The localization of Notch to the AJs was not markedly affected in either *O-fut1*^{R245A} (n = 28) or *shams* (n = 23) mutant cells (Fig. 5, *B–B‴* and *E–E‴*). However, Notch protein was severely reduced in the AJs of all double-mutant cells examined (n = 24), whereas the D*E*-cad staining appeared normal, suggesting that the AJ formation was not disrupted under these conditions (Fig. 5, *H–H‴*). Thus, monosaccharide *O*-fucose and the terminal dixylose of *O*-glucose-linked saccharides function redundantly in localizing Notch to the AJs. It has been suggested that Notch is first transported to the plasma membrane after synthesis, and then relocated to the AJs through transcytosis (48, 49). Thus, we speculated that relocation of Notch from the apical plasma membrane to the AJs might be prevented in the double-mutant cells. In contrast, Notch protein in the ER, detected by anti-protein-disulfide isomerase (PDI) antibody staining, appeared normal in *O-fut1*^{R245A} (n = 26) or *shams*-mutant (n = 28) cells and in *O-fut1*^{R245A} and *shams* double-mutant cells (n = 22) (Fig. 5, *C–C‴*, *F–F‴*, and *I–I‴*). Thus, Notch was normally exported from the ER in the absence of monosaccharide *O*-fucose and the terminal dixylose of *O*-glucose-linked saccharides (Fig. 5, *I–I‴*).

Distinct Functions of Monosaccharide O-Glucose and the Terminal Dixylose of O-Glucose-linked Saccharides in the Absence of Monosaccharide O-Fucose—In the *shams* mutant, the terminal dixylose is missing from the *O*-glucose trisaccha-

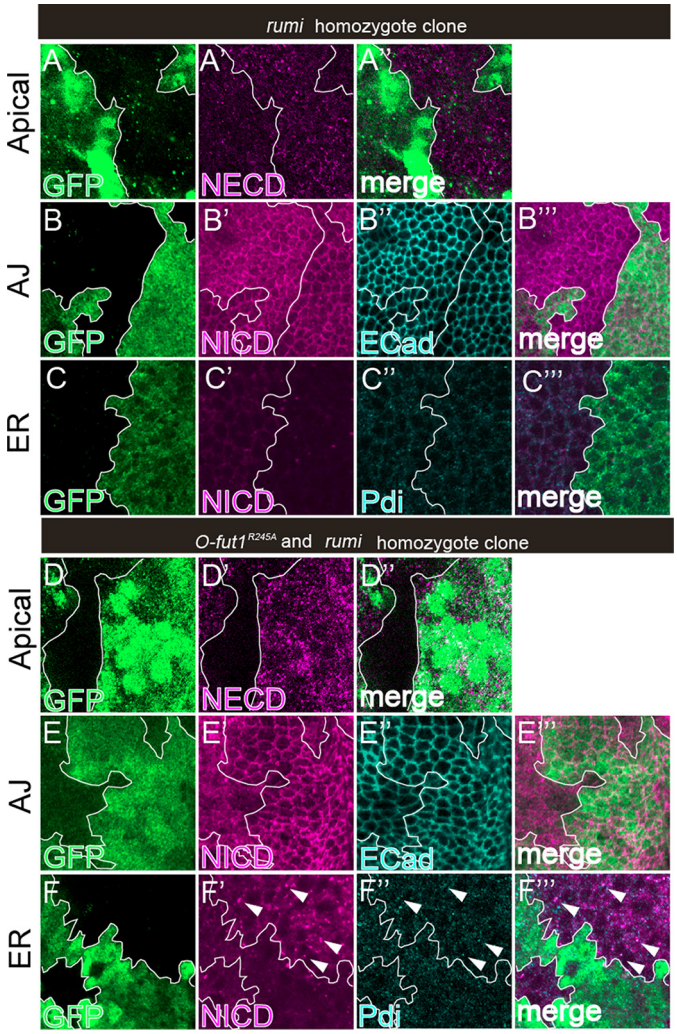

FIGURE 6. **Monosaccharide *O*-glucose and *O*-fucose play redundant roles in exporting Notch from the ER.** *A–F‴*, wing discs with somatic clones homozygous for *rumi*^{44}; *A–C‴*, or double-homozygous for *O-fut1*^{R245A} and *rumi*^{44}; *D–F‴* were stained with antibodies against NECD (*A′*, *A″*, *D′*, and *D″*); NICD (*B′*, *B‴*, *C′*, *C‴*, *E′*, *E‴*, *F′*, and *F‴*); DE-cad (B″ and *E″*); and PDI (*C″*, *C‴*, *F″*, and *F‴*). Optical images show planes corresponding to the apical membrane (*A–A″* and *D–D″*), AJs (*B–B‴* and *E–E*[tprime]), and the medial region including the ER (*C–C‴* and *F–F‴*). Note that NECD and NICD staining was absent from the apical membrane (*D′*) and AJs (*E′*), respectively, whereas NICD staining was increased and co-localized with PDI (*white arrowheads* in *F′–F‴*) in the *O-fut1*^{R245A} and *rumi*^{44} double-homozygous cells (lacking GFP). Mosaic clones of mutant cells are indicated by the absence of GFP. Clone boundaries are indicated by *white lines*. Wing discs were isolated from larvae raised at 25 °C. *A″*, *B‴*, *C‴*, *D″*, *E‴*, and *F‴* show merged images from *A–A′*, *B–B′*, *C–C″*, *D–D′*, *E–E′*, and *F–F″*, respectively.

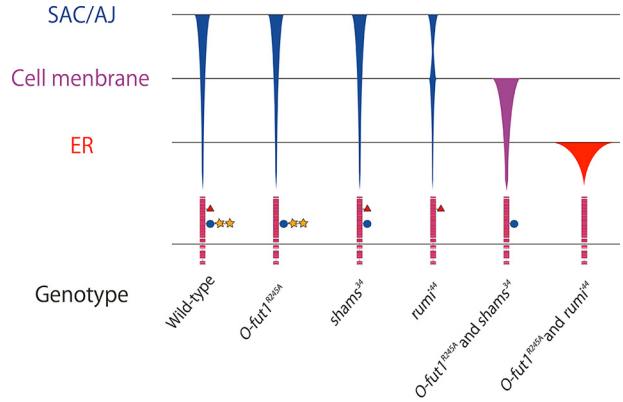

FIGURE 7. **Graphical representation of Notch distribution in each mutant.** Schematic showing the final destinations of Notch transport at 25 °C in various genotypes (indicated at the *bottom*). *SAC/AJ*, subapical complex/adherens junction. Symbols: *pink boxes*, EGF-like repeats; *red triangles*, *O*-fucosylation; *blue circles*, *O*-glucosylation; and *yellow stars*, xylose. The *thickness of the bars* qualitatively represents the amount of Notch protein at each location.

ride on the EGF-like repeats of Notch, although monosaccharide *O*-glucose is still present (13). Thus, we next examined whether Notch trafficking is affected differently by the absence of the terminal dixylose of *O*-glucose-linked saccharides *versus* the absence of monosaccharide *O*-glucose when Notch is not *O*-fucosylated. We generated somatic mosaics of *rumi*-mutant cells in which *O*-glucosylation of the Notch EGF-like repeats was abolished at 25 °C. In these cells, there was no marked difference in Notch detected at the apical plasma membrane (n = 31), the AJs (n = 42), or the ER (n = 26) (Fig. 6, *A–C‴*). In contrast, in *O-fut1*^{R245A} and *rumi* double-mutant cells, in which both monosaccharide *O*-fucose and *O*-glucose trisaccharide were missing, Notch was not detected at the apical plasma membrane (n = 18) or AJs (n = 20) at 25 °C in any of the cases examined (Fig. 6, *D–D″* and *E–E‴*). Thus, it is likely that the delivery of Notch to the plasma membrane fails under these conditions. We also observed that in all cases examined (n = 22), Notch accumulated in a portion of the ER in these double-mutant cells (Fig. 6, *F–F‴*, *arrowheads*). Thus, monosaccharide *O*-fucose and *O*-glucose trisaccharide share a redundant but essential function in exporting Notch from the ER. Interestingly, our results showed that in the absence of monosaccharide *O*-fucose, the Notch-trafficking defects caused by the absence of terminal dixylose of *O*-glucose-linked saccharides were different from those caused by the absence of monosaccharide *O*-glucose. Thus, not only are the *O*-glucose mono- and trisaccharide in part functionally redundant with the *O*-fucose monosaccharide, but the two types of *O*-glucose glycans also have roles that are distinct in terms of their contribution to Notch transport (Fig. 7).

Discussion

Multiple Glycan Modifications on a Protein May Have Redundant Roles—The EGF-like repeats in Notch contain multiple glycosylation sites to which specific and distinct sugars are added (8–16). Most studies of the specific functions of these glycans have drawn conclusions based on the consequences of the loss of a single sugar or a part of a single glycan chain. However, when multiple glycans have redundant functions, it is difficult to fully assess their functions using current approaches. In this study, we found that the terminal dixylose of *O*-glucose-linked saccharides and the monosaccharide *O*-fucose on Notch EGF-like repeats play redundant roles in Notch trafficking and activation.

A temperature-sensitive requirement of monosaccharide *O*-fucose in Notch signaling and transport has been observed in *Drosophila* (19). At a non-permissive temperature (30 °C), the monosaccharide *O*-fucose modification becomes essential for Notch signaling, and Notch lacking this modification accumulates in the ER (19); this effect is not observed at a permissive temperature (25 °C) (19). Similarly, in the absence of the terminal dixylose of *O*-glucose-linked saccharides, as observed in

Uxs or *shams* mutants, Notch signaling and transport were normal at 25 °C (Figs. 2, *F*, *I*, and *L*, 3*E*, and 5, *D*–*F*‴, and Fig. 4). However, importantly, the concurrent loss of the terminal dixylose of *O*-glucose-linked saccharides and monosaccharide *O*-fucose significantly reduced Notch signaling (Figs. 3*F* and 4). However, some Notch signaling was still present, because the number of SOPs increased even more markedly when the *Notch* gene was knocked down (Figs. 3*A* and 4). Nevertheless, it is clear that monosaccharide *O*-fucose and the terminal dixylose of *O*-glucose-linked saccharides function redundantly in Notch-signaling activation.

When both monosaccharide *O*-fucose and the terminal dixylose of *O*-glucose-linked saccharides were absent, Notch specifically accumulated at the apical plasma membrane and failed to localize to the AJs (Figs. 5, *G*–*I*‴, and 7). Thus, the reduction in Notch-signaling activity may be attributed to this mislocalization of Notch. However, the mechanism of this mislocalization is still unknown. It has been suggested that Notch is not directly transported to the AJs, but is instead relocated from the apical plasma membrane to the AJs by transcytosis (48, 49). Thus, the terminal dixylose of *O*-glucose-linked saccharides and the monosaccharide *O*-fucose may be crucial in facilitating the transcytosis of Notch. There are other cases in which the transcytosis of membrane proteins is required for relocation to their final position (50, 51). In mammalian neurons, the transcytosis of tropomyosin-related kinase A (TrkA) from the somatodendritic membrane is required for its specific localization to the axonal membrane (50, 51). TrkA has a terminal *N*-acetyllactosamine (LacNAc) on an *N*-linked glycan modification; galectin-4 binds the LacNAc and promotes the transcytosis of TrkA to the axonal membrane (50, 51). However, the molecular mechanisms of Notch transcytosis are not clear at present.

Multiple Roles of Notch O-Glucose Trisaccharide Glycan—We found that in the absence of monosaccharide *O*-fucose, the terminal dixylose of *O*-glucose-linked saccharides was required for relocating Notch from the apical plasma membrane to the AJs, whereas monosaccharide *O*-glucose was essential for exporting Notch from the ER (Figs. 5, *G*–*I*‴, 6, *D*–*F*‴, and 7). These results suggest that the *O*-glucose trisaccharide glycan has multiple functions in Notch trafficking, and that these distinct functions are complemented by monosaccharide *O*-fucose. Currently, the nature of these complex relationships between structure and function remains unclear. The *O*-fucose glycan on the EGF-like repeats of Notch has multiple roles in Notch signaling (9–11). Fringe adds GlcNAc to the monosaccharide *O*-fucose, thereby modifying the affinities of Notch for its ligands (11, 17). Monosaccharide *O*-fucose plays a sole and essential role in exporting Notch from the ER at a non-permissive temperature (19). Furthermore, in FGF signaling, FGF binds the GAG chain, which regulates its own signaling activity (52, 53). Removing specific regions of the GAG chain causes distinct defects in FGF signaling, suggesting that various GAG-chain regions have distinct biochemical roles (52, 53). Similarly, it is possible that monosaccharide *O*-glucose and the terminal dixylose of *O*-glucose-linked saccharides perform distinct biochemical functions to control Notch trafficking.

In this study, we demonstrated that two different *O*-glycan modifications on the EGF-like repeats of Notch have redundant roles. Because glycans in other protein motifs with multiple glycosylation sites may also function redundantly, analyzing glycan function by disrupting individual glycans may not be very informative. It is possible that a significant portion of information about the functions of glycan modifications is missing from previous studies that were based on the mutation analysis of single genes encoding a glycosyltransferase. To resolve this issue, it may be necessary to develop a systematic approach to disrupting multiple glycan structures.

Author Contributions—K. Matsumoto and K. Matsuno designed the research; K. Matsumoto, T. A., A. I., T. S., and T. Y. performed the research; K. Matsumoto and K. Matsuno analyzed the data; and K. Matsumoto and K. Matsuno wrote the paper.

Acknowledgments—We are grateful to Dr. Hamed Jafer-Nejad, Dr. Tom V. Lee, Dr. Tetsuya Tabata, Dr. Satoshi Goto, Dr. Miki Hino-Yamamoto, Dr. Shoko Nishihara, and Dr. Hideyuki Shimizu for helpful discussions and gifts of Drosophila stocks. We thank the Bloomington Stock Center, Vienna Drosophila resource center, and the Drosophila Genetic Resource Center for stocks, and the Developmental Studies Hybridoma Bank for antibodies.

References

1. Yamamoto, S., Charng, W. L., Rana, N. A., Kakuda, S., Jaiswal, M., Bayat, V., Xiong, B., Zhang, K., Sandoval, H., David, G., Wang, H., Haltiwanger, R. S., and Bellen, H. J. (2012) A mutation in EGF repeat-8 of Notch discriminates between Serrate/Jagged and Delta family ligands. *Science* **338,** 1229–1232
2. Luca, V. C., Jude, K. M., Pierce, N. W., Nachury, M. V., Fischer, S., and Garcia, K. C. (2015) Structural biology: structural basis for Notch1 engagement of Delta-like 4. *Science* **347,** 847–853
3. Pinho, S. S., and Reis, C. A. (2015) Glycosylation in cancer: mechanisms and clinical implications. *Nat. Rev. Cancer.* **15,** 540–555
4. Moremen, K. W., Tiemeyer, M., and Nairn, A. V. (2012) Vertebrate protein glycosylation: diversity, synthesis and function. *Nat. Rev. Mol. Cell. Biol.* **13,** 448–462
5. Stanley, P., and Okajima, T. (2010) Roles of glycosylation in Notch signaling. *Curr. Top. Dev. Biol.* **92,** 131–164
6. Chillakuri, C. R., Sheppard, D., Lea, S. M., and Handford, P. A. (2012) Notch receptor-ligand binding and activation: insights from molecular studies. *Semin. Cell Dev. Biol.* **23,** 421–428
7. Guruharsha, K. G., Kankel, M. W., and Artavanis-Tsakonas, S. (2012) The Notch signalling system: recent insights into the complexity of a conserved pathway. *Nat. Rev. Genet.* **13,** 654–666
8. Goto, S., Taniguchi, M., Muraoka, M., Toyoda, H., Sado, Y., Kawakita, M., and Hayashi, S. (2001) UDP-sugar transporter implicated in glycosylation and processing of Notch. *Nat. Cell Biol.* **3,** 816–822
9. Okajima, T., and Irvine, K. D. (2002) Regulation of notch signaling by *O*-linked fucose. *Cell* **111,** 893–904
10. Sasamura, T., Sasaki, N., Miyashita, F., Nakao, S., Ishikawa, H. O., Ito, M., Kitagawa, M., Harigaya, K., Spana, E., Bilder, D., Perrimon, N., and Matsuno, K. (2003) neurotic, a novel maternal neurogenic gene, encodes an *O*-fucosyltransferase that is essential for Notch-Delta interactions. *Development* **130,** 4785–4795
11. Moloney, D. J., Panin, V. M., Johnston, S. H., Chen, J., Shao, L., Wilson, R., Wang, Y., Stanley, P., Irvine, K. D., Haltiwanger, R. S., and Vogt, T. F. (2000) Fringe is a glycosyltransferase that modifies Notch. *Nature* **406,** 369–375
12. Acar, M., Jafar-Nejad, H., Takeuchi, H., Rajan, A., Ibrani, D., Rana, N. A., Pan, H., Haltiwanger, R. S., and Bellen, H. J. (2008) Rumi is a CAP10

domain glycosyltransferase that modifies Notch and is required for Notch signaling. *Cell* **132,** 247–258
13. Lee, T. V., Sethi, M. K., Leonardi, J., Rana, N. A., Buettner, F. F., Haltiwanger, R. S., Bakker, H., and Jafar-Nejad, H. (2013) Negative regulation of notch signaling by xylose. *PLoS Genet.* **9,** e1003547
14. Sakaidani, Y., Nomura, T., Matsuura, A., Ito, M., Suzuki, E., Murakami, K., Nadano, D., Matsuda, T., Furukawa, K., and Okajima, T. (2011) *O*-Linked *N*-acetylglucosamine on extracellular protein domains mediates epithelial cell-matrix interactions. *Nat. Commun.* **2,** 583
15. Boskovski, M. T., Yuan, S., Pedersen, N. B., Goth, C. K., Makova, S., Clausen, H., Brueckner, M., and Khokha, M. K. (2013) The heterotaxy gene GALNT11 glycosylates Notch to orchestrate cilia type and laterality. *Nature* **504,** 456–459
16. Takeuchi, H., Fernández-Valdivia, R. C., Caswell, D. S., Nita-Lazar, A., Rana, N. A., Garner, T. P., Weldeghiorghis, T. K., Macnaughtan, M. A., Jafar-Nejad, H., and Haltiwanger, R. S. (2011) Rumi functions as both a protein *O*-glucosyltransferase and a protein *O*-xylosyltransferase. *Proc. Natl. Acad. Sci. U.S.A.* **108,** 16600–16605
17. Okajima, T., Xu, A., and Irvine, K. D. (2003) Modulation of notch-ligand binding by protein *O*-fucosyltransferase 1 and fringe. *J. Biol. Chem.* **278,** 42340–42345
18. Okajima, T., Xu, A., Lei, L., and Irvine, K. D. (2005) Chaperone activity of protein *O*-fucosyltransferase 1 promotes Notch receptor folding. *Science* **307,** 1599–1603
19. Ishio, A., Sasamura, T., Ayukawa, T., Kuroda, J., Ishikawa, H. O., Aoyama, N., Matsumoto, K., Gushiken, T., Okajima, T., Yamakawa, T., and Matsuno, K. (2015) *O*-Fucose monosaccharide of *Drosophila* Notch has a temperature-sensitive function and cooperates with *O*-glucose glycan in Notch transport and Notch signaling activation. *J. Biol. Chem.* **290,** 505–519
20. Ryder, E., Ashburner, M., Bautista-Llacer, R., Drummond, J., Webster, J., Johnson, G., Morley, T., Chan, Y. S., Blows, F., Coulson, D., Reuter, G., Baisch, H., Apelt, C., Kauk, A., Rudolph, T., *et al*. (2007) The DrosDel deletion collection: a *Drosophila* genomewide chromosomal deficiency resource. *Genetics* **177,** 615–629
21. Mummery-Widmer, J. L., Yamazaki, M., Stoeger, T., Novatchkova, M., Bhalerao, S., Chen, D., Dietzl, G., Dickson, B. J., and Knoblich, J. A. (2009) Genome-wide analysis of Notch signalling in *Drosophila* by transgenic RNAi. *Nature* **458,** 987–992
22. Ueyama, M., Takemae, H., Ohmae, Y., Yoshida, H., Toyoda, H., Ueda, R., and Nishihara, S. (2008) Functional analysis of proteoglycan galactosyltransferase II RNA interference mutant flies. *J. Biol. Chem.* **283,** 6076–6084
23. Rincón-Limas, D. E., Lu, C. H., Canal, I., Calleja, M., Rodríguez-Esteban, C., Izpisúa-Belmonte, J. C., and Botas, J. (1999) Conservation of the expression and function of apterous orthologs in *Drosophila* and mammals. *Proc. Natl. Acad. Sci. U.S.A.* **96,** 2165–2170
24. Micchelli, C. A., The, I., Selva, E., Mogila, V., and Perrimon, N. (2002) Rasp, a putative transmembrane acyltransferase, is required for Hedgehog signaling. *Development* **129,** 843–851
25. Ray, M., and Lakhotia, S. C. (2015) The commonly used eye-specific sev-GAL4 and GMR-GAL4 drivers in *Drosophila melanogaster* are expressed in tissues other than eyes also. *J. Genet.* **94,** 407–416
26. Guo, M., Jan, L. Y., and Jan, Y. N. (1996) Control of daughter cell fates during asymmetric division: interaction of Numb and Notch. *Neuron* **17,** 27–41
27. Hummel, T., and Klämbt, C. (2008) P-element mutagenesis. *Methods Mol. Biol.* **420,** 97–117
28. Ayukawa, T., Matsumoto, K., Ishikawa, H. O., Ishio, A., Yamakawa, T., Aoyama, N., Suzuki, T., and Matsuno, K. (2012) Rescue of Notch signaling in cells incapable of GDP-L-fucose synthesis by gap junction transfer of GDP-L-fucose in *Drosophila*. *Proc. Natl. Acad. Sci. U.S.A.* **109,** 15318–15323
29. Takei, Y., Ozawa, Y., Sato, M., Watanabe, A., and Tabata, T. (2004) Three *Drosophila* EXT genes shape morphogen gradients through synthesis of heparan sulfate proteoglycans. *Development* **131,** 73–82
30. Ishikawa, H. O., Ayukawa, T., Nakayama, M., Higashi, S., Kamiyama, S., Nishihara, S., Aoki, K., Ishida, N., Sanai, Y., and Matsuno, K. (2010) Two pathways for importing GDP-fucose into the endoplasmic reticulum lumen function redundantly in the *O*-fucosylation of Notch in *Drosophila*. *J. Biol. Chem.* **285,** 4122–4129
31. Kuroda, J., Nakamura, M., Yoshida, M., Yamamoto, H., Maeda, T., Taniguchi, K., Nakazawa, N., Hatori, R., Ishio, A., Ozaki, A., Shimaoka, S., Ito, T., Iida, H., Okumura, T., Maeda, R., and Matsuno, K. (2012) Canonical Wnt signaling in the visceral muscle is required for left-right asymmetric development of the *Drosophila* midgut. *Mech. Dev.* **128,** 625–639
32. Hoskins, R. A., Landolin, J. M., Brown, J. B., Sandler, J. E., Takahashi, H., Lassmann, T., Yu, C., Booth, B. W., Zhang, D., Wan, K. H., Yang, L., Boley, N., Andrews, J., Kaufman, T. C., Graveley, B. R., *et al*. (2011) Genome-wide analysis of promoter architecture in *Drosophila melanogaster*. *Genome Res.* **21,** 182–192
33. Dang, D. T., and Perrimon, N. (1992) Use of a yeast site-specific recombinase to generate embryonic mosaics in *Drosophila*. *Dev. Genet.* **13,** 367–375
34. Lacroix, C., Giovannini, D., Combe, A., Bargieri, D. Y., Späth, S., Panchal, D., Tawk, L., Thiberge, S., Carvalho, T. G., Barale, J. C., Bhanot, P., and Ménard, R. (2011) FLP/FRT-mediated conditional mutagenesis in pre-erythrocytic stages of *Plasmodium berghei*. *Nat. Protoc.* **6,** 1412–1428
35. Okajima, T., Reddy, B., Matsuda, T., and Irvine, K. D. (2008) Contributions of chaperone and glycosyltransferase activities of *O*-fucosyltransferase 1 to Notch signaling. *BMC Boil.* **6,** 1
36. Bar-Peled, M., Griffith, C. L., and Doering, T. L. (2001) Functional cloning and characterization of a UDP-glucuronic acid decarboxylase: the pathogenic fungus *Cryptococcus neoformans* elucidates UDP-xylose synthesis. *Proc. Natl. Acad. Sci. U.S.A.* **98,** 12003–12008
37. Eixelsberger, T., Sykora, S., Egger, S., Brunsteiner, M., Kavanagh, K. L., Oppermann, U., Brecker, L., and Nidetzky, B. (2012) Structure and mechanism of human UDP-xylose synthase: evidence for a promoting role of sugar ring distortion in a three-step catalytic conversion of UDP-glucuronic acid. *J. Biol. Chem.* **287,** 31349–31358
38. Eames, B. F., Singer, A., Smith, G. A., Wood, Z. A., Yan, Y. L., He, X., Polizzi, S. J., Catchen, J. M., Rodriguez-Mari, A., Linbo, T., Raible, D. W., and Postlethwait, J. H. (2010) UDP xylose synthase 1 is required for morphogenesis and histogenesis of the craniofacial skeleton. *Dev. Biol.* **341,** 400–415
39. Bakker, H., Oka, T., Ashikov, A., Yadav, A., Berger, M., Rana, N. A., Bai, X., Jigami, Y., Haltiwanger, R. S., Esko, J. D., and Gerardy-Schahn, R. (2009) Functional UDP-xylose transport across the endoplasmic reticulum/Golgi membrane in a Chinese hamster ovary cell mutant defective in UDP-xylose synthase. *J. Biol. Chem.* **284,** 2576–2583
40. Götting, C., Kuhn, J., Zahn, R., Brinkmann, T., and Kleesiek, K. (2000) Molecular cloning and expression of human UDP-D-xylose:proteoglycan core protein β-D-xylosyltransferase and its first isoform XT-II. *J. Mol. Biol.* **304,** 517–528
41. Kamimura, K., Koyama, T., Habuchi, H., Ueda, R., Masu, M., Kimata, K., and Nakato, H. (2006) Specific and flexible roles of heparan sulfate modifications in *Drosophila* FGF signaling. *J. Cell Biol.* **174,** 773–778
42. Couso, J. P., and Martinez Arias, A. (1994) Notch is required for wingless signaling in the epidermis of *Drosophila*. *Cell* **79,** 259–272
43. The, I., and Perrimon, N. (2000) Morphogen diffusion: the case of the wingless protein. *Nat. Cell Biol.* **2,** E79–82
44. Han, C., Belenkaya, T. Y., Khodoun, M., Tauchi, M., Lin, X., and Lin, X. (2004) Distinct and collaborative roles of *Drosophila* EXT family proteins in morphogen signalling and gradient formation. *Development* **131,** 1563–1575
45. Franch-Marro, X., Wendler, F., Guidato, S., Griffith, J., Baena-Lopez, A., Itasaki, N., Maurice, M. M., and Vincent, J. P. (2008) Wingless secretion requires endosome-to-Golgi retrieval of Wntless/Evi/Sprinter by the retromer complex. *Nat. Cell Biol.* **10,** 170–177
46. Port, F., Kuster, M., Herr, P., Furger, E., Bänziger, C., Hausmann, G., and Basler, K. (2008) Wingless secretion promotes and requires retromer-dependent cycling of Wntless. *Nat. Cell Biol.* **10,** 178–185
47. Frise, E., Knoblich, J. A., Younger-Shepherd, S., Jan, L. Y., and Jan, Y. N. (1996) The *Drosophila* Numb protein inhibits signaling of the Notch re-

ceptor during cell-cell interaction in sensory organ lineage. *Proc. Natl. Acad. Sci. U.S.A.* **93,** 11925–11932
48. Sasaki, N., Sasamura, T., Ishikawa, H. O., Kanai, M., Ueda, R., Saigo, K., and Matsuno, K. (2007) Polarized exocytosis and transcytosis of Notch during its apical localization in *Drosophila* epithelial cells. *Genes Cells* **12,** 89–103
49. Sasamura, T., Ishikawa, H. O., Sasaki, N., Higashi, S., Kanai, M., Nakao, S., Ayukawa, T., Aigaki, T., Noda, K., Miyoshi, E., Taniguchi, N., and Matsuno, K. (2007) The *O*-fucosyltransferase *O*-fut1 is an extracellular component that is essential for the constitutive endocytic trafficking of Notch in *Drosophila*. *Development* **134,** 1347–1356
50. Watson, F. L., Porcionatto, M. A., Bhattacharyya, A., Stiles, C. D., and Segal, R. A. (1999) TrkA glycosylation regulates receptor localization and activity. *J. Neurobiol.* **39,** 323–336
51. Abad-Rodríguez, J., and Diez-Revuelta, N. (2015) Axon glycoprotein routing in nerve polarity, function, and repair. *Trends Biochem. Sci.* **40,** 385–396
52. Forsten-Williams, K., Chua, C. C., and Nugent, M. A. (2005) The kinetics of FGF-2 binding to heparan sulfate proteoglycans and MAP kinase signaling. *J. Theor. Biol.* **233,** 483–499
53. Pan, Y., Woodbury, A., Esko, J. D., Grobe, K., and Zhang, X. (2006) Heparan sulfate biosynthetic gene *Ndst1* is required for FGF signaling in early lens development. *Development* **133,** 4933–4944